

A reserve stem cell population in small intestine renders *Lgr5*-positive cells dispensable

Hua Tian¹, Brian Biehs², Søren Warming¹, Kevin G. Leong³, Linda Rangell⁴, Ophir D. Klein² & Frederic J. de Sauvage¹

The small intestine epithelium renews every 2 to 5 days, making it one of the most regenerative mammalian tissues. Genetic inducible fate mapping studies have identified two principal epithelial stem cell pools in this tissue. One pool consists of columnar *Lgr5*-expressing cells that cycle rapidly and are present predominantly at the crypt base¹. The other pool consists of *Bmi1*-expressing cells that largely reside above the crypt base². However, the relative functions of these two pools and their interrelationship are not understood. Here we specifically ablated *Lgr5*-expressing cells in mice using a human diphtheria toxin receptor (*DTR*) gene knocked into the *Lgr5* locus. We found that complete loss of the *Lgr5*-expressing cells did not perturb homeostasis of the epithelium, indicating that other cell types can compensate for the elimination of this population. After ablation of *Lgr5*-expressing cells, progeny production by *Bmi1*-expressing cells increased, indicating that *Bmi1*-expressing stem cells compensate for the loss of *Lgr5*-expressing cells. Indeed, lineage tracing showed that *Bmi1*-expressing cells gave rise to *Lgr5*-expressing cells, pointing to a hierarchy of stem cells in the intestinal epithelium. Our results demonstrate that *Lgr5*-expressing cells are dispensable for normal intestinal homeostasis, and that in the absence of these cells, *Bmi1*-expressing cells can serve as an alternative stem cell pool. These data provide the first experimental evidence for the interrelationship between these populations. The *Bmi1*-expressing stem cells may represent both a reserve stem cell pool in case of injury to the small intestine epithelium and a source for replenishment of the *Lgr5*-expressing cells under non-pathological conditions.

Two types of stem cells have been described in the small intestine based on location and cycling dynamics^{1–4}. Fast-cycling stem cells express markers including *Lgr5*, *Cd133* (also known as *Prom1*) and *Sox9* (refs 1, 5, 6) and are present throughout the intestine. Also known as crypt base columnar cells (CBCs), these slender cells populate the crypt and villi within 3 days, and are interspersed among the Paneth cells that support them^{7,8}. Slower-cycling stem cells, marked by enriched expression of *Bmi1* or mouse *Tert* (*mTert*), represent a rarer cell population^{2,9}. These cells form a descending gradient from proximal to distal regions of the intestine, such that they are more prevalent in the duodenum than in the colon. Despite their rarity, *Bmi1*-expressing stem cells are crucial for crypt maintenance².

To study the function of *Lgr5*-expressing cells, we replaced the first coding exon of *Lgr5* with two distinct cassettes. The first consisted of a dsRED-IRES-CreERT2 sequence to enable genetic lineage tracing studies by tamoxifen (TAM)-inducible expression of Cre in *Lgr5*-expressing cells (Supplementary Fig. 1a, *Lgr5*^{CreER} allele). The second cassette contained enhanced green fluorescent protein (EGFP) linked in frame to a human DTR cDNA (Supplementary Fig. 1a, *Lgr5*^{DTR} allele), producing a fusion protein. Consistent with previous reports¹, one injection of TAM in *Lgr5*^{CreER};R26R mice marked *Lgr5*-expressing stem cells in a mosaic fashion and led to generation of labelled progeny for more than 60 days (Supplementary Fig. 1b). Expression of DTR-EGFP

in *Lgr5*^{DTR} mice functioned as a reporter for *Lgr5* expression (Fig. 1a) and also conferred diphtheria toxin (DT) sensitivity on CBCs. Expression of EGFP in mice carrying the *Lgr5*^{DTR} allele was detected at the membrane of cycling CBCs in every crypt (Supplementary Fig. 1c–e, CBCs are marked by asterisks).

We next set out to test the effects of eliminating *Lgr5*-expressing cells by administering DT to *Lgr5*^{DTR} mice. Twenty-four hours after DT administration, all EGFP-positive cells were depleted, including CBCs (Fig. 1a, b, j, k, p, q). Loss of *Lgr5*-expressing cells was further confirmed by the absence of *Lgr5* messenger RNA (Fig. 1d, e) and was accompanied by extensive apoptosis at the base of the crypts, with shedding of dead cells into the lumen (Fig. 1m, n).

After sustained DT exposure for 10 days, both the EGFP reporter and *Lgr5* mRNA were completely absent from the base of the crypts (Fig. 1c, f and Supplementary Fig. 2) but, notably, crypt architecture was comparable to controls (Fig. 1g, i, j, l). Proliferating CBCs were absent from the crypt (Fig. 1l, r), such that the crypt base was occupied mostly or entirely by Paneth cells (Supplementary Fig. 3a, b). The extensive apoptosis detected 24 h after DT treatment had significantly decreased by day 10 (compare Fig. 1n with o) but was still detectable. No increase in crypt fission after DT treatment was observed by haematoxylin and eosin staining at any time point (Fig. 1g–i).

Because *Lgr5*-expressing cells have been proposed to have a critical role in renewal of the intestine, it was surprising that the architecture of the intestinal epithelium was essentially intact after ablation of *Lgr5*-expressing CBCs (Fig. 1g–i). Within the villi, very little change in the total number of endocrine cells was observed (Supplementary Fig. 3c, d), and goblet cells were abundant in the crypts and villi (Supplementary Fig. 3g, h, j). Upon CBC ablation, Paneth cells were found at the bottom of the crypts and in some cases were mislocalized to the villi (Supplementary Fig. 3a, b and data not shown); additionally, migration of cells as assessed by BrdU pulse-chase labelling was normal (Supplementary Fig. 4). The only major difference from controls that we observed was in the secretory cell lineage; the number of chromogranin-A-positive enteroendocrine cells in the crypts doubled after DT administration for 10 days (Supplementary Fig. 3e, f, i).

We did not detect any *Lgr5*-expressing CBCs using either the EGFP reporter or *in situ* hybridization after 10 days of DT (Fig. 1c, f and Supplementary Fig. 2), but it was still possible that a few CBCs could have escaped ablation and repopulated the epithelium, as a similar scenario was reported in *c-Myc* and *Ascl2* conditional null mice^{10,11}. To address this possibility directly, we visualized *Lgr5*-expressing cell activity during DT selection by producing *Lgr5*^{DTR/CreER};R26R mice. These mutant mice carried two null alleles at the *Lgr5* locus, of which one enabled ablation of *Lgr5*-expressing cells and the other enabled lineage tracing of any possibly remaining *Lgr5*-expressing cells. These mice died at postnatal day (P)1, consistent with previous reports that *Lgr5* null mice are not viable¹². To analyse the postnatal gut, we grew pieces of small intestine from embryonic day (E)15 *Lgr5*^{DTR/CreER};R26R embryos under the kidney capsule of immunocompromised mice for

¹Department of Molecular Biology, Genentech Inc., 1 DNA Way, South San Francisco, California 94080, USA. ²Departments of Orofacial Sciences and Pediatrics, Institute for Human Genetics and Program in Craniofacial and Mesenchymal Biology, UCSF, 513 Parnassus Avenue, San Francisco, California 94143-0442, USA. ³Department of Research Oncology, Genentech Inc., 1 DNA Way, South San Francisco, California 94080, USA. ⁴Department of Pathology, Genentech Inc., 1 DNA Way, South San Francisco, California 94080, USA.

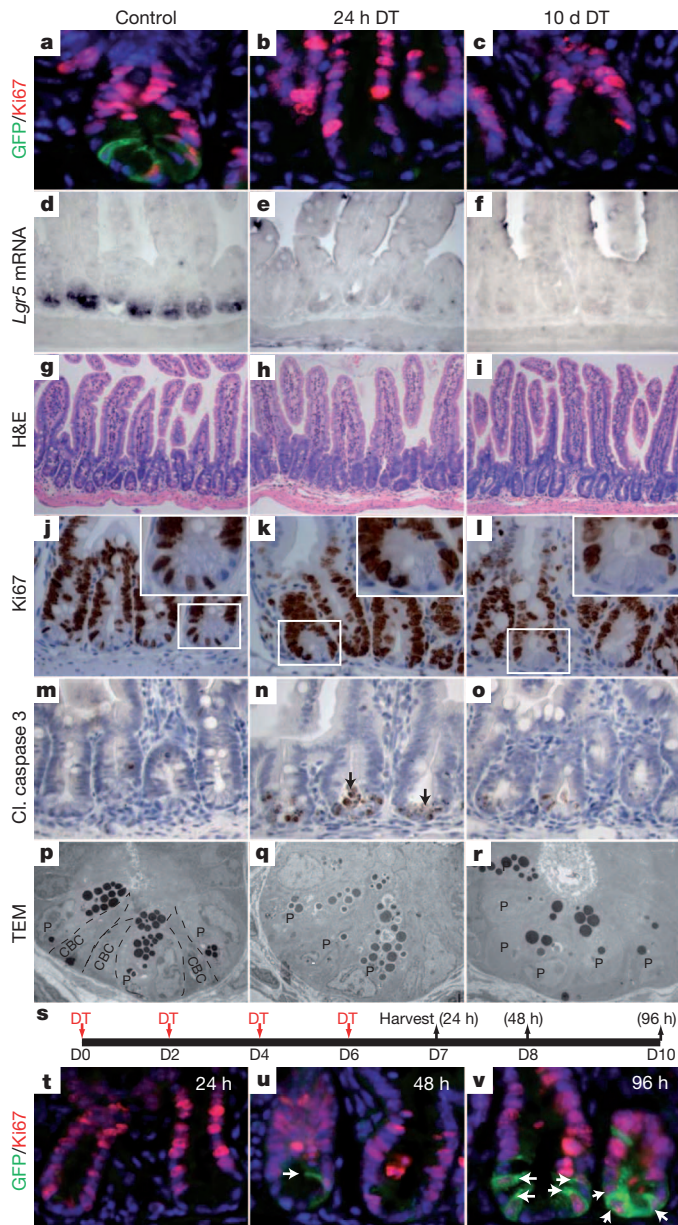


Figure 1 | Characterization of DT-mediated CBC ablation. **a**, EGFP is detected on the membrane of Ki67⁺ proliferating CBCs in saline-treated *Lgr5*^{DTR/+} mice. **b**, One dose of DT eliminates all DTR-EGFP-positive cells at 24 h. **c**, DT treatment for up to 10 days prevents reappearance of *Lgr5*-expressing cells. **d–f**, *Lgr5* mRNA is normally present at the bottom of the crypts (**d**) and is not detected after 24 h (**e**) or 10 days of DT treatment (**f**). **g–i**, Crypt architecture is intact after ablation of *Lgr5*-expressing CBCs. H&E, haematoxylin and eosin. **j–l**, Proliferation above the crypt base is normal after ablation of *Lgr5*-expressing CBCs. **m–o**, Extensive apoptosis is observed at the crypt base 24 h after DT and tapers off by 10 days, but is still higher than controls. ‘Cl. caspase 3’ is cleaved caspase 3. **p–r**, Electron microscopy shows that CBCs in controls are characterized by slender nuclei and scant cytoplasm. No CBCs remain at the crypt base after one dose or 10 days of DT treatment. The crypt base is filled with granule-rich Paneth cells. TEM, transmission electron microscopy. **s**, Dosing regimen for study of the recovery of *Lgr5*-expressing CBCs. **t**, No CBCs are detected 24 h after DT administration. **u**, A few *Lgr5*⁺/Ki67⁺ CBCs (arrow) were detected 48 h after the last dose of DT. **v**, More *Lgr5*⁺/Ki67⁺ CBCs (arrows) recovered after 96 h. Original magnification for panels: **a–f**, **m–o** and **t–v** at 40 \times ; **g–i** at 20 \times ; **j–l** at 63 \times ; and **p–r** at 2,650 \times .

three weeks, at which point they formed crypts comparable to P17 intestine (Fig. 2a–e)¹³. After 10 days of TAM treatment, columns of blue cells emanated from the crypt base, and progeny of *Lgr5*-expressing cells differentiated into all four major cell types of the intestinal

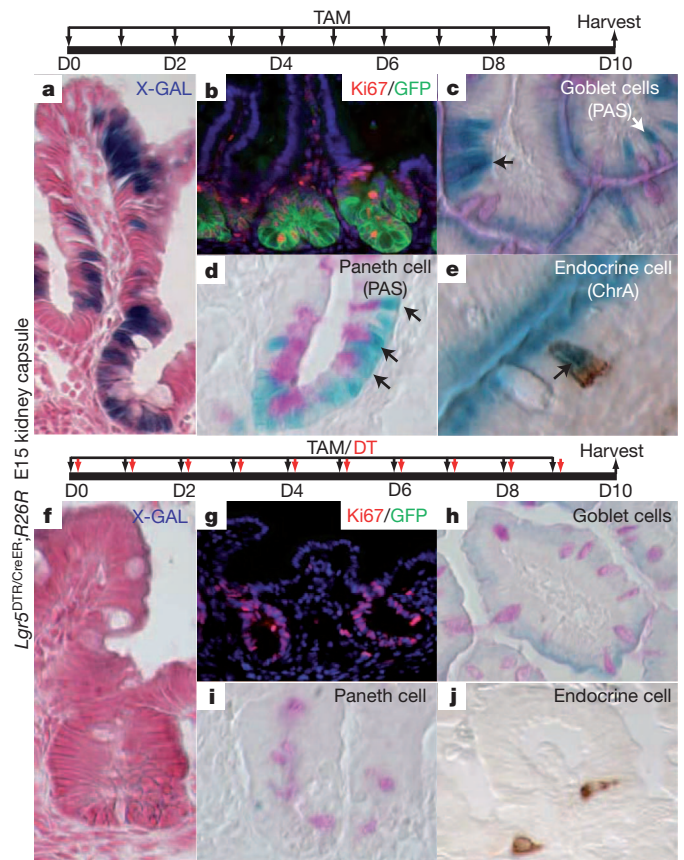


Figure 2 | Maintenance of normal crypt architecture is not mediated by *Lgr5*-positive cells that have escaped ablation. **a**, Ten-day lineage tracing of descendants of *Lgr5*-expressing stem cells shows a blue ribbon emanating from the base of the crypt in a grafted intestine piece from E15 *Lgr5*^{DTR/CreER} embryos. **b–e**, Normal proliferation and differentiation of intestinal epithelium after loss of *Lgr5* gene function. *Lgr5*-expressing stem cells can give rise to all four major differentiated cell types (arrows). X-GAL-positive cells mark *Lgr5*-positive stem cell progeny, which overlap with differentiated cell markers for goblet (**c**), Paneth (**d**) and endocrine cell (**e**) lineages. PAS, periodic acid Schiff; ChrA, Chromogranin A. **f**, Concurrent TAM and DT treatment kills all *Lgr5*-expressing cells. No progeny of *Lgr5*-expressing cells (blue) are detected in the grafted intestine. **g–j**, No GFP-positive cells are detected but proliferation and differentiation are normal after DT-mediated ablation of *Lgr5*-expressing CBCs. Original magnification for panels: **a**, **b**, **f**, **g** at 40 \times ; **c–e**, **h–j** at 63 \times .

epithelium (Fig. 2a–e). Concomitant administration of DT and TAM for 10 days eradicated all EGFP-positive CBCs (Fig. 2g), and no cells descended from *Lgr5*-expressing cells were observed (Fig. 2f), confirming that the *Lgr5*^{DTR} allele leads to complete elimination of these cells. Importantly, no abnormalities in graft morphology, differentiation or proliferation were observed in these mice compared to controls (Fig. 2a–j).

Although *Lgr5*-expressing cells were completely depleted within 24 h of DT treatment, persistence of apoptotic bodies at the crypt base throughout the 10-day DT treatment suggested that *Lgr5*-expressing CBCs were continuously generated and eliminated during the treatment (Fig. 1n, o). This notion was supported by the quick recovery of *Lgr5*-expressing cells between 48 to 96 h after the final dose of DT (Fig. 1s–v). To follow the fate of the newly generated *Lgr5*-expressing cells, mice implanted with *Lgr5*^{DTR/CreER};R26R embryonic intestine fragments in the kidney capsule were allowed to recover for 6 days in the presence of TAM following 6 days of DT treatment. A row of blue cells emanated from the crypt base (Supplementary Fig. 5a), indicating that the newly formed *Lgr5*-expressing stem cells (Supplementary Fig. 5b, GFP-positive cells) gave rise to progeny that migrated out of the crypt. When the converse experiment was performed by

injecting TAM for 6 days and then dosing with DT from days 6 to 12, blue cells were only present in the upper region of the villi (Supplementary Fig. 5c), indicating that progeny of *Lgr5*-expressing cells marked between day 1 and 6 migrated out of the crypts into the villi, but that during DT treatment between days 6 and 12, *Lgr5*-expressing stem cells were no longer available (Supplementary Fig. 5d, absence of GFP signal) to supply labelled (blue) progeny to replenish the epithelium.

To study the long-term effects of CBC ablation, we isolated crypts from *Lgr5*^{DTR/+} mice to perform *in vitro* crypt organoid cultures¹⁴. Crypts depleted of *Lgr5*-expressing CBCs by treatment for 10 days with DT, as indicated by absence of GFP expression, gave rise to organoids with similar efficiency as wild-type controls (Supplementary Fig. 6a, b). These could be passaged *in vitro* in DT for up to 2 months without losing their ability to expand and proliferate. No *Lgr5*-expressing (GFP-positive) cells were detected in organoid epithelium as long as the organoids were maintained in medium containing DT (Supplementary Fig. 6d). However, when DT was removed from the culture medium, *Lgr5*-expressing cells reappeared at the bottom of crypt-like structures within 3 days (Supplementary Fig. 6c, GFP-positive cells).

Because we found that *Lgr5*-expressing CBCs were dispensable for crypt maintenance, we next asked whether *Bmi1*-expressing stem cells were mobilized to compensate for the loss of *Lgr5*-expressing stem cells. Mouse BMI1 regulates self-renewal of haematopoietic and neuronal stem cells¹⁵. We used a GFP knock-in allele (*Bmi1*^{GFP/+}) to monitor *Bmi1* gene expression¹⁶. *Bmi1*-expressing GFP-positive cells were most commonly observed at positions 3 to 6 above the crypt base (Fig. 3a), consistent with the *Bmi1* mRNA expression pattern in the small intestine². Upon depletion of *Lgr5*-expressing CBCs in *Lgr5*^{DTR/+}; *Bmi1*^{GFP/+} mice after 9 days of DT treatment, the number of GFP-positive cells per crypt increased three fold (Fig. 3a–d and Supplementary Fig. 7a), and the proportion of crypts containing either single or multiple GFP-expressing cells increased by 40% compared to control animals (Supplementary Fig. 7b). Of note, 55% of the total number of GFP-positive crypts in *Lgr5*^{DTR/+}; *Bmi1*^{GFP/+} mice now contained multiple GFP-positive cells (Fig. 3d and Supplementary Fig. 7b), compared with only 22% in *Bmi1*^{GFP/+} control animals.

To trace the fate of cells descended from *Bmi1*-expressing cells after elimination of *Lgr5*-expressing CBCs, we generated a *Bmi1*CreER bacterial artificial chromosome (BAC) transgenic allele (Supplementary Fig. 8). Labelling kinetics using the *Bmi1*-CreER transgenic line crossed with the R26R reporter were identical to previously reported results using the *Bmi1*^{CreER} knock-in allele² (Fig. 3f). *Bmi1*-CreER;R26R;*Lgr5*^{DTR/+} animals were treated with alternating doses of DT and TAM per day for 7 days (Fig. 3e). Because *Bmi1*-expressing cells are most abundant in the first 5 cm of the duodenum, we focused our analysis on this region. Consistent with the increased number of *Bmi1*-expressing cells (Supplementary Fig. 7a), the proportion of LacZ-positive crypts (either partially or fully labelled) also increased 34% upon loss of *Lgr5*-expressing CBCs (Supplementary Fig. 7c). The most marked difference was in the number of fully labelled crypts. Only 2.3% of crypts were fully labelled in *Bmi1*CreER;R26R control mice during a 6-day lineage tracing period, which was comparable with previous studies using a *Bmi1*^{CreER} knock-in allele². Upon loss of *Lgr5*-expressing CBCs, the number of fully labelled crypts increased approximately 15-fold (Fig. 3h, i and Supplementary Fig. 7c). These results indicate that in the absence of *Lgr5*-expressing cells, *Bmi1*-expressing cells are capable of directly giving rise to all intestinal cell types without going through *Lgr5*-positive intermediate cells. However, *Bmi1*-expressing stem cells did not give rise to an increased number of labelled crypts in more distal regions of small intestine and colon upon loss of *Lgr5*-expressing CBCs (Fig. 3f, g), indicating that alternative stem cell pools must compensate for the loss of *Lgr5*-expressing stem cells in distal regions of the gut.

Lastly, we tested whether *Bmi1*-expressing cells give rise to *Lgr5*-expressing cells under normal conditions. Because *Bmi1*- and *Lgr5*-expressing cells represent distinct although overlapping cell populations, we carried out a series of short-term pulse-chase experiments

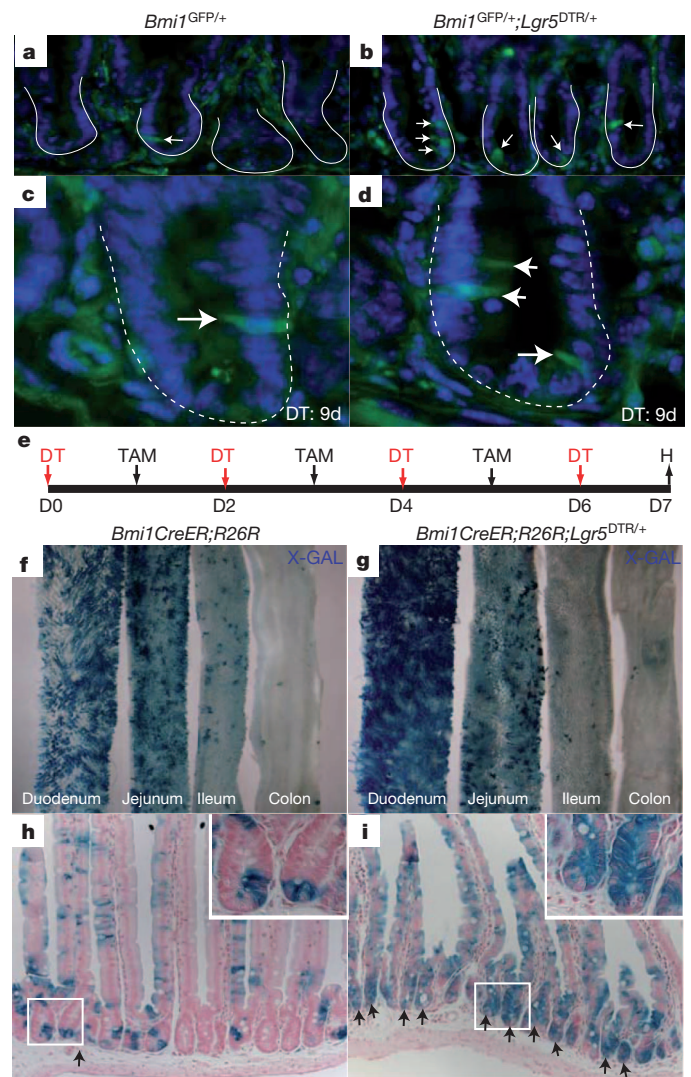
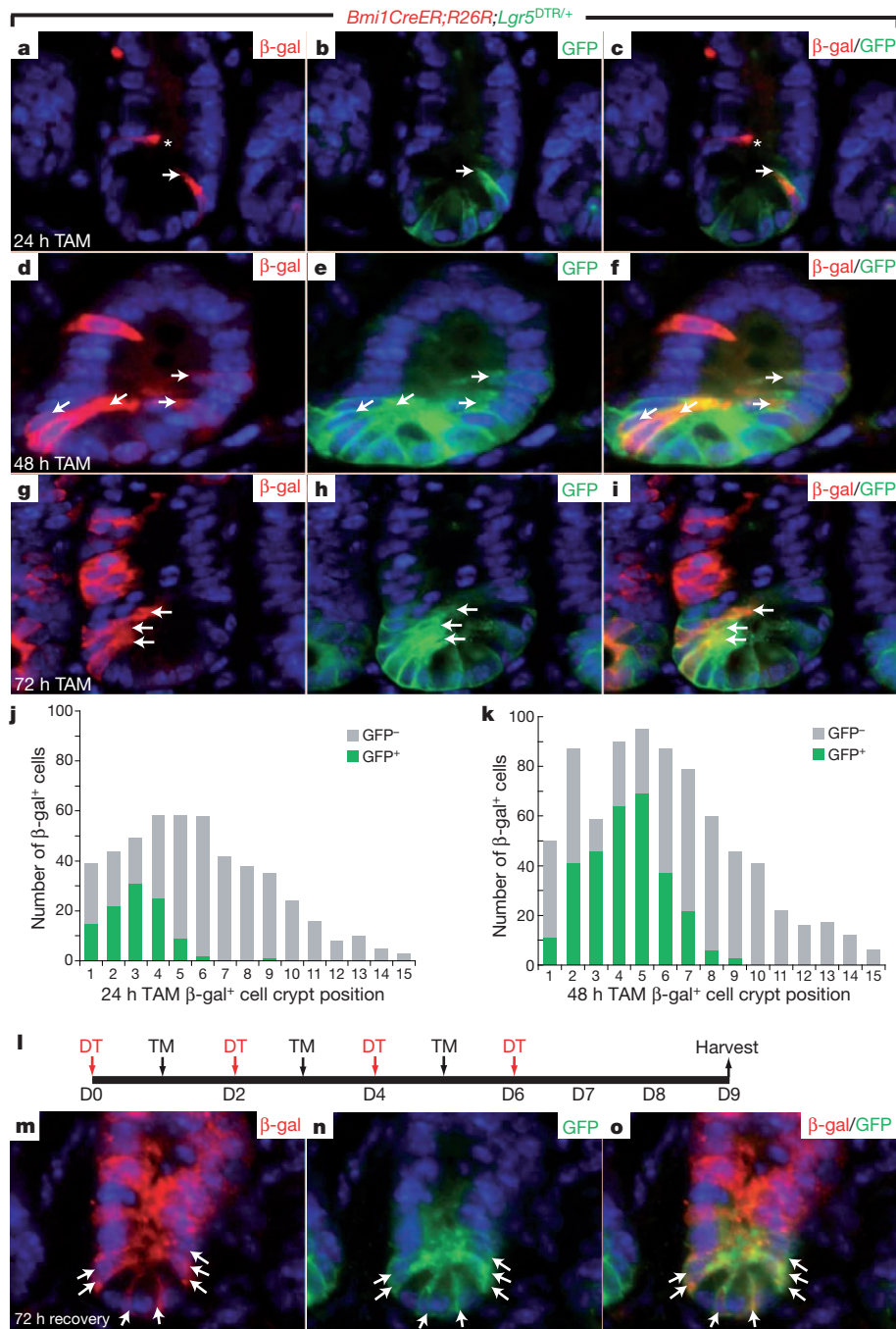


Figure 3 | *Bmi1*-expressing stem cells are mobilized to compensate for the loss of *Lgr5*-expressing CBCs. **a**, Rare *Bmi1*-expressing cells (arrows) are detected at positions 3 to 6 of the crypt base in the duodenum of *Bmi1*^{GFP/+} reporter mice. **b**, Increased *Bmi1*-expressing cells appear at the crypt base upon ablation of *Lgr5*-expressing CBCs. **c**, Higher magnification showing a *Bmi1*-expressing cell at position 4 of crypt base in *Bmi1*^{GFP/+} reporter mice. **d**, Close-up view of a crypt with multiple *Bmi1*-expressing cells after ablation of *Lgr5*-expressing cells. Arrows in **a–d** indicate (*Bmi1*)-expressing cells. **e**, Dosing regimen for lineage tracing of *Bmi1*-expressing cell progeny after ablation of *Lgr5*-expressing CBCs. H, harvest. **f, g**, Whole-mount X-GAL staining of the gastrointestinal tract. In both control mice and after ablation of *Lgr5*-expressing CBCs, *Bmi1*-expressing cells produce more progeny in the proximal than in the distal intestine. **h, i**, Close-up view of X-GAL-positive crypts in duodenum. Most of the labelled crypts have less than five X-GAL-positive cells in *Bmi1*-CreER;R26R control animals. Ablation of *Lgr5*-expressing CBCs stimulates production of progeny by *Bmi1*-expressing cells. 36% of the crypts in the first 5 cm of duodenum now become fully labelled (marked by arrows). Original magnification for panels: **a–d** at 40 \times ; **f, g** at 1.2 \times ; **h, i** at 20 \times .

using *Bmi1*-CreER;R26R;*Lgr5*^{DTR/+} mice. Twenty-four hours after TAM administration, most of the β -galactosidase (β -gal)-positive cells appeared as individuals, reflecting the normal pattern of *Bmi1* expression (Fig. 4a) in the initially labelled cells. *Bmi1*-expressing cells (β -gal positive) overlapped with *Lgr5*-expressing cells (GFP positive) between positions 1 to 6 at the crypt base; the double-positive cells peaked at positions 3 and 4 (Fig. 4a–c). This observation is consistent with a previous report stating that *Bmi1* mRNA expression (via quantitative polymerase chain reaction (qPCR) analysis) was readily detectable in *Lgr5*-positive cells¹¹. Later, between 48–72 h, clonal expansion



from *Bmi1*-expressing cells was evident, as β -gal/GFP double-positive cells now appeared as doublets or triplets (Fig. 4d–i). We scored a total of 500 crypts at each time point and found that although a few cells were β -gal/GFP double positive (that is, expressing both *Bmi1* and *Lgr5*) at 24 h after TAM induction, this number doubled at 48 h (Fig. 4j, k). Similarly, lineage tracing from *Bmi1*-expressing cells carried out in mice treated for 6 days with DT and allowed to recover

expressing CBCs (arrow). **j, k**, Distribution of the *Bmi1*-positive stem cell progeny (β -gal⁺ cells) within the crypt at 24 and 48 h after TAM induction. **j**, *Bmi1*-expressing cells appear as singles throughout the crypt base between positions 1 to 15. **k**, More cells are derived from *Bmi1*-expressing stem cells at 48 h. A significant portion of β -gal⁺ cells also express *Lgr5* (GFP⁺, green column), at positions 1 to 6. Overlapping cells (green) peak around positions 3, 4 or 5. **l**, Dosing regimen used to study the recovery of *Lgr5*-expressing CBCs from *Bmi1*-positive cells. **m–o**, *Bmi1*-positive cells give rise to a fully labelled crypt (red), including newly formed *Lgr5*-expressing CBCs (GFP⁺, arrows). The original magnification for all panels is 40 \times .

for 72 h (Fig. 4l) demonstrated that newly formed *Lgr5*-positive cells at the bottom of the crypts arose from *Bmi1*-expressing cells (Fig. 4m–o). Together, these data show that *Bmi1*-expressing cells can give rise to *Lgr5*-expressing cells both under normal physiological conditions and after insults that deplete CBCs. Similar to our observation, *mTert*-expressing stem cells could also give rise to *Lgr5*-positive cells over a 5-day lineage tracing period⁹.

Our data support the existence of two stem cell pools in the epithelium of the small intestine: an actively proliferating stem cell compartment responsible for the daily maintenance of the intestine epithelium that is characterized by the expression of *Lgr5*, *Ascl2* and *Olfm4* (refs 1, 11, 17) and a distinct pool of stem cells expressing *Bmi1*. Our results lend support to the two-stem-cell pool model that is based on computational approaches¹⁸, and provide experimental evidence for recent models predicting that the intestine could fully recover after complete elimination of cellular subpopulations deemed to be functional stem cells¹⁹. Our data do not support the recent proposal that *Bmi1*-expressing cells are exclusively a subset of *Lgr5*-expressing cells¹¹; rather they indicate that under normal circumstances, *Bmi1*-positive stem cells are upstream of rapidly cycling, *Lgr5*-expressing stem cells and replenish the pool of active stem cells, either to avoid exhaustion of actively cycling stem cells or to prevent the accumulation of damaged cells that may lead to the development of tumours. Importantly, we also demonstrate that when the *Lgr5*-expressing cell compartment is eliminated by DT treatment, *Bmi1*-expressing cells can increase in number, presumably as a compensatory mechanism. Under these conditions, *Bmi1*-expressing cells contribute directly to the generation of all cell types of the intestinal epithelium to produce a functional organ until the rapidly cycling stem cell compartment is able to recover. Although it has been proposed that *Bmi1*-expressing stem cells are quiescent², this remains to be conclusively demonstrated.

Distinct stem cell pools with differing cycling dynamics have previously been observed in the hair follicle and in blood, organs that, like the intestine, undergo regular bouts of proliferation and regeneration^{20–22}. The factors that regulate the interplay between discrete populations of stem cells, and the precise hierarchical relationships among such populations, remain to be characterized. Although we have found that loss of *Lgr5*-positive cells is sustainable under short-term conditions *in vivo*, it remains to be determined whether such a scenario can persist for longer periods of time. Interestingly, depletion of Paneth cells, which are thought to be important for the maintenance of CBCs⁷, can be tolerated by mice for over 6 months without significant structural defects of the epithelium^{23,24}, supporting the idea that the intestine can function normally in the absence of CBCs. It will be important to determine how different stem cell populations sense the activity of other populations, whether rapidly cycling cells can repopulate more quiescent stem cell populations, and whether additional subpopulations of stem cells exist.

METHODS SUMMARY

Mice. *Lgr5*^{DTR/+}, *Lgr5*^{CreER/+} and *Bmi1*-*CreER* alleles were generated as described in Methods. *Bmi1*^{GFP/+} mice were provided by I. Weissman¹⁶. All studies and procedures involving animal subjects were approved by the Institutional Animal Care and Use Committees of Genentech and the University of California, San Francisco, and were conducted strictly in accordance with the approved animal handling protocol.

Full Methods and any associated references are available in the online version of the paper at www.nature.com/nature.

Received 19 April; accepted 1 August 2011.

Published online 18 September 2011.

1. Barker, N. *et al.* Identification of stem cells in small intestine and colon by marker gene *Lgr5*. *Nature* **449**, 1003–1007 (2007).
2. Sangiorgi, E. & Capecchi, M. R. *Bmi1* is expressed *in vivo* in intestinal stem cells. *Nature Genet.* **40**, 915–920 (2008).

3. Li, L. & Clevers, H. Coexistence of quiescent and active adult stem cells in mammals. *Science* **327**, 542–545 (2010).
4. Fuchs, E. The tortoise and the hair: slow-cycling cells in the stem cell race. *Cell* **137**, 811–819 (2009).
5. Zhu, L. *et al.* Prominin 1 marks intestinal stem cells that are susceptible to neoplastic transformation. *Nature* **457**, 603–607 (2009).
6. Furuyama, K. *et al.* Continuous cell supply from a Sox9-expressing progenitor zone in adult liver, exocrine pancreas and intestine. *Nature Genet.* **43**, 34–41 (2011).
7. Sato, T. *et al.* Paneth cells constitute the niche for *Lgr5* stem cells in intestinal crypts. *Nature* **469**, 415–418 (2011).
8. Cheng, H. & Leblond, C. P. Origin, differentiation and renewal of the four main epithelial cell types in the mouse small intestine. V. Unitarian Theory of the origin of the four epithelial cell types. *Am. J. Anat.* **141**, 537–561 (1974).
9. Montgomery, R. K. *et al.* Mouse telomerase reverse transcriptase (mTert) expression marks slowly cycling intestinal stem cells. *Proc. Natl Acad. Sci. USA* **108**, 179–184 (2011).
10. Muncan, V. *et al.* Rapid loss of intestinal crypts upon conditional deletion of the Wnt/Tcf-4 target gene *c-Myc*. *Mol. Cell. Biol.* **26**, 8418–8426 (2006).
11. van der Flier, L. G. *et al.* Transcription factor achaete scute-like 2 controls intestinal stem cell fate. *Cell* **136**, 903–912 (2009).
12. Garcia, M. I. *et al.* LGR5 deficiency deregulates Wnt signaling and leads to precocious Paneth cell differentiation in the fetal intestine. *Dev. Biol.* **331**, 58–67 (2009).
13. Crosnier, C., Stamatakis, D. & Lewis, J. Organizing cell renewal in the intestine: stem cells, signals and combinatorial control. *Nature Rev. Genet.* **7**, 349–359 (2006).
14. Sato, T. *et al.* Single *Lgr5* stem cells build crypt-villus structures *in vitro* without a mesenchymal niche. *Nature* **459**, 262–265 (2009).
15. Park, I. K., Morrison, S. J. & Clarke, M. F. *Bmi1*, stem cells, and senescence regulation. *J. Clin. Invest.* **113**, 175–179 (2004).
16. Hosen, N. *et al.* *Bmi-1*-green fluorescent protein-knock-in mice reveal the dynamic regulation of *bmi-1* expression in normal and leukemic hematopoietic cells. *Stem Cells* **25**, 1635–1644 (2007).
17. van der Flier, L. G., Haegerbarth, A., Stange, D. E., van de Wetering, M. & Clevers, H. OLFM4 is a robust marker for stem cells in human intestine and marks a subset of colorectal cancer cells. *Gastroenterology* **137**, 15–17 (2009).
18. Lobachevsky, P. N. & Radford, I. R. Intestinal crypt properties fit a model that incorporates replicative ageing and deep and proximate stem cells. *Cell Prolif.* **39**, 379–402 (2006).
19. Buske, P. *et al.* A comprehensive model of the spatio-temporal stem cell and tissue organisation in the intestinal crypt. *PLoS Comput. Biol.* **7**, e1001045 (2011).
20. Wilson, A. *et al.* Hematopoietic stem cells reversibly switch from dormancy to self-renewal during homeostasis and repair. *Cell* **135**, 1118–1129 (2008).
21. Ito, M. *et al.* Stem cells in the hair follicle bulge contribute to wound repair but not to homeostasis of the epidermis. *Nature Med.* **11**, 1351–1354 (2005).
22. Hsu, Y. C., Pasolli, H. A. & Fuchs, E. Dynamics between stem cells, niche, and progeny in the hair follicle. *Cell* **144**, 92–105 (2011).
23. Bastide, P. *et al.* Sox9 regulates cell proliferation and is required for Paneth cell differentiation in the intestinal epithelium. *J. Cell Biol.* **178**, 635–648 (2007).
24. Garabedian, E. M., Roberts, L. J., McNevin, M. S. & Gordon, J. I. Examining the role of Paneth cells in the small intestine by lineage ablation in transgenic mice. *J. Biol. Chem.* **272**, 23729–23740 (1997).

Supplementary Information is linked to the online version of the paper at www.nature.com/nature.

Acknowledgements We gratefully acknowledge efforts by all the members of the Genentech mouse facility, in particular R. Ybarra and G. Morrow. We are grateful to N. Strauli, D.-K. Tran and A. Rathnayake for assistance with mouse breeding. We thank M. Roose-Girma, X. Rairdan and the members of the embryonic stem cell and microinjection groups for embryonic stem cell work and transgenic line generation and members of the F.J.d.S. laboratory for discussions and ideas. This work was funded in part by the National Institutes of Health through the NIH Director's New Innovator Award Program, 1-DP2-OD007191 and by R01-DE021420, both to O.D.K.

Author Contributions H.T., B.B., S.W., K.G.L. and L.R. designed, performed experiments and collected data. H.T., B.B., O.D.K. and F.J.d.S. designed experiments, analysed the data and wrote the manuscript. O.D.K. and F.J.d.S. are joint senior authors. All authors discussed results and edited the manuscript.

Author Information Reprints and permissions information is available at www.nature.com/reprints. The authors declare competing financial interests: details accompany the full-text HTML version of the paper at www.nature.com/nature. Readers are welcome to comment on the online version of this article at www.nature.com/nature. Correspondence and requests for materials should be addressed to F.J.d.S. (desauvage.fred@gene.com) or O.D.K. (ophir.klein@ucsf.edu).

METHODS

***Lgr5* and *Bmi1* vector construction.** The constructs for targeting the C57BL/6 *Lgr5* locus and the *Bmi1* BAC transgene were made using a combination of recombineering, DNA synthesis and standard molecular cloning techniques^{25,26}.

For *Lgr5*, a 7,213 bp fragment (assembly NCBI37/mm9, chr10:115,020,315-115,027,527) from a C57BL/6 BAC (RP23 library) was first retrieved into plasmid pBlight-TK²⁵. To generate the DTR-EGFP KI vector for *Lgr5*, a DTR-EGFP-pA-loxP-Neo-loxP cassette was synthesized (Blue Heron/Origene, DTR-EGFP sequence was based on that described previously²⁷, and inserted right after the ATG of *Lgr5* (chr10:115,024,547, reverse strand), deleting the remainder of exon 1 and splice donor of intron 1 (a 212 bp deletion). To generate the CreERT2 KI vector, a dsRed2-IRES-CreERT2-pA-Frt-neo-Frt cassette was synthesized (Blue Heron/Origene) and inserted at the same position as the DTR-EGFP cassette. The final vectors were confirmed by DNA sequencing.

The *Lgr5* KI vectors were linearized with NotI and C57BL/6 C2 embryonic stem cells were targeted using standard methods (G418-positive and gancyclovir-negative selection). Positive clones were identified using PCR and taqman analysis, and confirmed by sequencing of the modified locus. Correctly targeted embryonic stem cells were transfected with a Cre or Flpe plasmid, respectively, to remove the Neo cassette. The modified embryonic stem cells were then injected into blastocysts using standard techniques, and germline transmission was obtained after crossing the resulting chimaeras with C57BL/6N females.

For *Bmi1*, a 210 kb C57BL/6 BAC (RP23-181D14, assembly NCBI37/mm9, chr2:18,464,619-18,674,471) was obtained and characterized by DNA fingerprinting. The BAC contains the *Bmi1* locus and considerable 5' and 3' flanking sequence. An IRES-CreERT2-pA-frt-Neo-frt cassette was synthesized (Blue Heron/Origene) and inserted, using recombineering, 85 bp 3' of the *Bmi1* stop codon (after position chr2:18,606,193). Neo was then removed by transforming the modified BAC into arabinose-induced, SW105 cells^{28,29} expressing the yeast protein Flp. C57BL/6 transgenic mice carrying the modified *Bmi1* BAC were obtained using standard pronuclear microinjection methods³⁰ and characterized.

We analysed the *Lgr5*^{DTR/+} mice at 24 h after DT administration (50 µg kg⁻¹, intraperitoneal injection, *n* = 3), at 10 days of DT treatment (50 µg kg⁻¹ every other day for 10 days, *n* = 5), 48 h recovery (*n* = 3) and 96 h recovery time points after four doses of DT (*n* = 2). The DT treatment could not be extended beyond 10 days due to severe liver toxicity apparently mediated by a subset of *Lgr5*-DTR-EGFP-expressing hepatocytes. We analysed *Bmi1*CreER;R26R;*Lgr5*^{DTR/+} at 24 h (*n* = 2), 48 h (*n* = 2) and 72 h (*n* = 2) after TAM injection. Two-hundred and fifty β-gal-positive crypts were scored per mouse.

Renal capsule explants. 3–5-mm small intestine pieces from E15 *Lgr5*^{DTR/CreER} embryos (*n* = 3) were grafted under the renal capsule of 6–8-week-old athymic nu/nu mice and allowed to develop for 3 weeks. We treated *Lgr5*^{DTR/CreER};R26R renal grafts with 10 days TAM (*n* = 5), 10 days DT/TAM (*n* = 5), 6 days DT followed by 6 days TAM (*n* = 5) and 6 days TAM followed by 6 days DT

(*n* = 5). Some GFP expression was seen outside of the CBC region due to perdurance of GFP protein as well as upregulation of the *Lgr5* locus when *Lgr5* is deleted¹². **DT cell ablation.** Mice (between 6 and 12 weeks old) were given DT at 50 µg kg⁻¹ every 48 h through intraperitoneal injections.

TAM labelling experiments. Mice (between 6 and 12 weeks old) were given 5 mg TAM in corn oil through intraperitoneal injection.

Transmission electron microscopy. The tissues were fixed in 1/2 Karnovsky's fixative (2% paraformaldehyde (PFA), 2.5% glutaraldehyde in 0.1 M sodium cacodylate buffer, pH 7.2), washed in the same buffer, and post-fixed in 1% osmium tetroxide. The samples were then dehydrated through a series of ethanol, followed by propylene oxide and embedded in Eponate 12 (Ted Pella). Thin sections were stained with uranyl acetate and lead citrate and examined using a Philips CM12 or JEOL JEM-1400 TEM.

Histology, immunohistochemistry and immunofluorescence. Animals were perfused with 2% PFA. Small intestine and colon were flushed with 2% PFA and fixed in 4% PFA overnight. Half of the materials were cryo-protected, embedded in OCT, and sectioned at 6 µm for immunofluorescence. The other half of the materials were paraffin embedded, sectioned at 3 µm for histology and immunohistochemistry. Antibodies: Ki67 (Neomarker), cleaved caspase 3 (Cell Signaling), GFP (Novus), chromogranin A (Neomarkers), β-gal (Cappel).

In situ hybridization and X-GAL staining. Full-length *Lgr5* cDNA was cloned into the pGEM vector to make anti-sense DIG-probe. Protocols for *in vitro* transcription and *in situ* hybridization were as described previously³¹. Whole-mount X-GAL staining was performed as described².

Crypt organoid culture. Crypt isolation and culture were performed as described¹⁴.

- Warming, S., Rachel, R. A., Jenkins, N. A. & Copeland, N. G. *Zfp423* is required for normal cerebellar development. *Mol. Cell Biol.* **26**, 6913–6922 (2006).
- Liu, P., Jenkins, N. A. & Copeland, N. G. A highly efficient recombineering-based method for generating conditional knockout mutations. *Genome Res.* **13**, 476–484 (2003).
- Kissenpfennig, A. *et al.* Dynamics and function of Langerhans cells *in vivo*: dermal dendritic cells colonize lymph node areas distinct from slower migrating Langerhans cells. *Immunity* **22**, 643–654 (2005).
- Warming, S., Costantino, N., Court, D. L., Jenkins, N. A. & Copeland, N. G. Simple and highly efficient BAC recombineering using galK selection. *Nucleic Acids Res.* **33**, e36 (2005).
- Lee, E. C. *et al.* A highly efficient *Escherichia coli*-based chromosome engineering system adapted for recombinogenic targeting and subcloning of BAC DNA. *Genomics* **73**, 56–65 (2001).
- Van Keuren, M. L., Gavriliina, G. B., Filipiak, W. E., Zeidler, M. G. & Saunders, T. L. Generating transgenic mice from bacterial artificial chromosomes: transgenesis efficiency, integration and expression outcomes. *Transgenic Res.* **18**, 769–785 (2009).
- Gregorieff, A. & Clevers, H. *In situ* hybridization to identify gut stem cells. *Curr. Protoc. Stem Cell Biol.* Ch. 2, Unit 2F.1 (2010).